



## Formation and magnetic properties of Fe–Pt alloy clusters by plasma-gas condensation

D. L. Peng, T. Hihara, and K. Sumiyama

Citation: *Applied Physics Letters* **83**, 350 (2003); doi: 10.1063/1.1592301

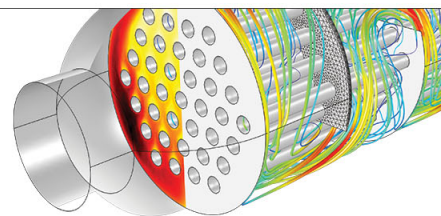
View online: <http://dx.doi.org/10.1063/1.1592301>

View Table of Contents: <http://scitation.aip.org/content/aip/journal/apl/83/2?ver=pdfcov>

Published by the [AIP Publishing](#)

---

Over **700** papers &  
presentations on  
multiphysics simulation



VIEW NOW ►

 COMSOL

## Formation and magnetic properties of Fe–Pt alloy clusters by plasma-gas condensation

D. L. Peng,<sup>a)</sup> T. Hihara, and K. Sumiyama

*Department of Materials Science and Engineering, Nagoya Institute of Technology,  
Nagoya 466-8555, Japan*

(Received 17 March 2003; accepted 28 May 2003)

Size-monodispersed  $\text{Fe}_x\text{Pt}_{1-x}$  alloy clusters were synthesized using a plasma-gas-condensation technique which employs two separate elemental sputtering sources and a growth chamber. The composition of the alloy clusters was controlled by adjusting the ratio of the applied sputtering power. We found that high-temperature disordered fcc- $\text{Fe}_x\text{Pt}_{1-x}$  clusters whose mean diameters of 6–9 nm depend on the Ar gas flow ratio were formed for a wide average composition range ( $x \approx 0.3$ – $0.7$ ), and the lattice constant of as-deposited clusters increases almost linearly with decreasing  $x$ , being extrapolated to the value of pure Pt metal. For  $\text{Fe}_{49}\text{Pt}_{51}$  cluster-assembled films, high coercivity (8.8 kOe) was obtained by annealing at 600 °C within 10 min due to improved chemical ordering, although as-deposited cluster-assembled films have lower blocking temperatures than room temperature, and show a small coercivity value ( $\sim 25$  Oe) at room temperature due to intercluster magnetic interaction. © 2003 American Institute of Physics.

[DOI: 10.1063/1.1592301]

There has been a growing interest in the nanostructurally tailored materials because they are expected to become the basic infrastructure of next-generation devices.<sup>1</sup> In these material designs, nanometer-sized particles or clusters serves as elemental functional units. Thus, a key to the success of this technology is an ability to control geometrical and chemical structures of nanometer-scale clusters. With the decrease of the memory unit size, on the other hand, superparamagnetism becomes a serious problem because the magnetization direction is eliminated by thermal fluctuation. Recently, as a promising material for hard-disk drives with ultrahigh recording density,  $L1_0$  structured FePt based nonocomposite films<sup>2–4</sup> and chemically synthesized FePt-self-assembled nanoparticles<sup>5–7</sup> have attracted much attention since it is well known that equiatomic FePt alloy has extremely high magnetic anisotropy energy,  $K_u$  ( $\sim 10^7$  J/m<sup>3</sup>). However, little work has been done on the Fe–Pt cluster-assembled system by vapor-phase synthesis method.<sup>8</sup>

In this letter, we report formation and magnetic properties of Fe–Pt alloy clusters produced by the plasma-gas-condensation method. We obtained size-monodispersed Fe–Pt alloy clusters with a high-temperature disordered fcc structure, although from an application point of view, formation of as-deposited alloy clusters with the room-temperature ordered structure ( $L1_0$ ) is highly desired. However, we find that the high anisotropy  $L1_0$  FePt phase was obtained by annealing at 600 °C within 10 min.

Since metal vapors are produced by sputtering of a target material, a wide variety of elements can serve as source materials.<sup>9</sup> We prepared the samples by using the plasma-gas-condensation-type cluster beam deposition apparatus,<sup>10,11</sup> which is based on plasma-glow-discharge vaporization (sputtering) and inert gas condensation techniques. The apparatus is composed of the three main parts: a

sputtering chamber, a cluster growth room, and a deposition chamber. We used a magnetron sputtering system with Fe and Pt targets of 80 mm in diameter, controlled independently for the generation of metal vapors. The two targets were placed face to face, separated by 100 mm. The input power of each target was controlled in the range of 50–150 W. A large amount of Ar gas of 300–400 sccm was introduced continuously into the sputtering chamber, making the pressure inside the chamber approximately 1.5–1.7 Torr. The vaporized Fe and Pt atoms in the sputtering chamber are decelerated by collisions with Ar gas and are swept into the cluster growth room, which is cooled by liquid nitrogen. The clusters formed in this room are ejected from a small nozzle by differential pumping and a part of the cluster beam is intercepted by a skimmer, and then deposited onto a sample holder in the deposition chamber ( $10^{-5}$ – $10^{-4}$  Torr).

We used two kinds of substrates for the Fe–Pt cluster deposition: carbon-coated colodion films supported by Cu microgrids for transmission electron microscopy (TEM) observation and quartz plates for magnetic measurements. We used a Hitachi HF-2000 TEM operating at 200 kV for structural characterization. This microscope was equipped with energy-dispersive x-ray (EDX) spectroscopy, which was used for compositional analyses. Magnetic measurement was performed using a superconducting quantum interference device magnetometer between 5 and 300 K in magnetic fields up to 50 kOe. The effective film thickness of deposited clusters,  $t_e$ , was estimated using a quartz crystal thickness monitor, which measures the weight of the deposited clusters. Heat treatment of as-deposited samples was carried out in a gas pressure of about  $2 \times 10^{-6}$  Torr and with a heating rate is 30 °C min<sup>-1</sup>.

Figure 1(a) shows bright-field TEM images and the size distributions of the clusters with effective thickness  $t_e \approx 2.5$  nm prepared at  $R_{\text{Ar}}=400$  sccm when the power of Pt was fixed to 150 W, while that of Fe was varied from (a) 90,

<sup>a)</sup>Electronic mail: pengdl@mse.nitech.ac.jp

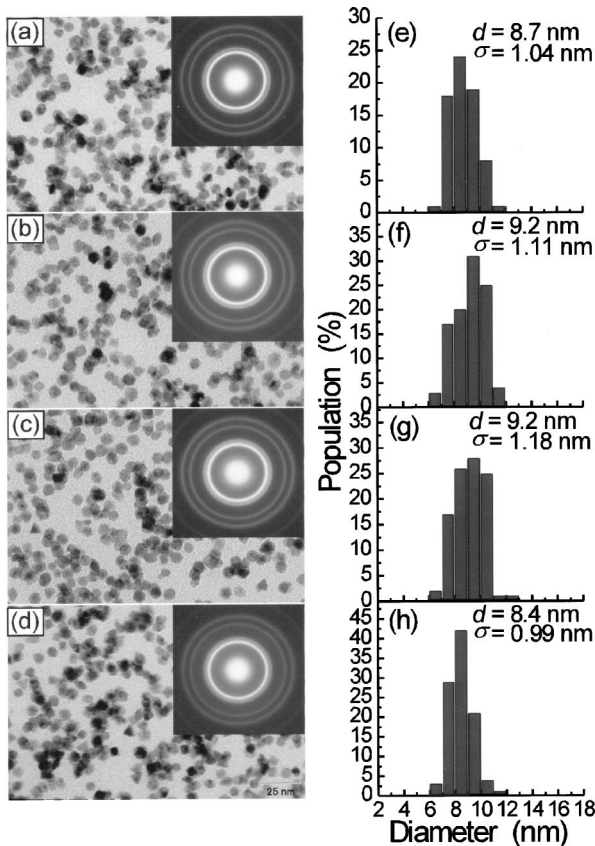


FIG. 1. (a), (b), (c), (d) Bright-field TEM images and electron diffraction patterns (insets) of  $\text{Fe}_x\text{Pt}_{1-x}$  alloy clusters, and (e), (f), (g), (h) size distribution of the clusters shown on the left, corresponding to Fe content of  $x = 39\%$ ,  $49\%$ ,  $55\%$ , and  $69\%$ , respectively. Ar gas flow rate:  $R_{\text{Ar}} = 400$  sccm; sputtering powers: Pt target 150 W (fixed), and Fe target: (a) 90, (b) 105, (c) 110, and (d) 130 W.

(b) 105, (c) 110, to (d) 130 W, corresponding to Fe content of 39%, 49%, 55%, and 69%, respectively. The electron diffraction (ED) patterns (insets) observed for cluster assemblies with  $t_e \approx 30$  nm can be ascribed to high-temperature disordered fcc Fe–Pt alloy phase. This result suggests that the nonequilibrium nature of Fe–Pt alloy cluster formation in the vapor phase, being the same with the observation results for the Fe–Pt alloy films<sup>3,12,13</sup> or nanoparticles<sup>5–7</sup> obtained by other methods.

The plan-view and cross-sectional scanning electron microscopy observations (not shown here) show that most of the clusters have a ball-like shape. Using an image-analysis software (Image-Pro PLUS: Media Cybernetics), we estimated the size distributions [Figs. 1(e), 1(f), 1(g), 1(h)] of the clusters which do not touch and overlap each other in the digitized images recorded by a slow scan charge coupled device camera in the object area of  $350 \times 350$  nm<sup>2</sup>. As shown here, the mean cluster diameter,  $d$ , is about 9 nm and the standard deviations ( $\sigma$ ) are less than 12% of  $d$  for these samples.

The composition of individual clusters with  $d \approx 9$  nm was also analyzed for the average composition of 52.5 at. % Fe. We randomly selected 36 different clusters and took the EDX spectra by nanoelectron beams. The estimated compositions are shown as a histogram in Fig. 2. The chemical compositions of these clusters exhibit a narrow peak at  $\sim 52.5$  at. % Fe, being consistent with the average composi-

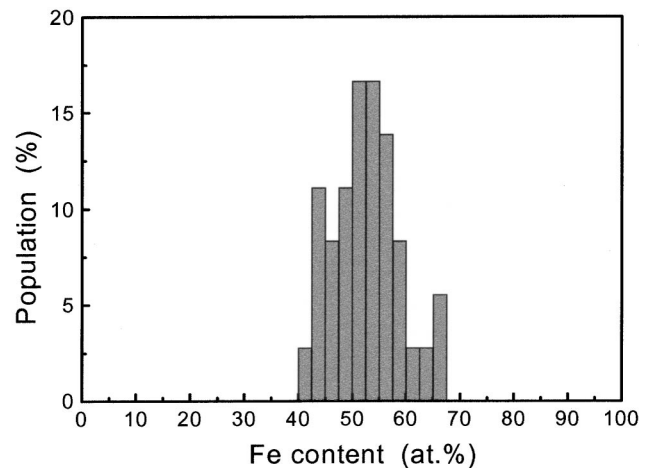


FIG. 2. A chemical composition histogram evaluated from the nanobeam EDX spectra of 36 individual Fe–Pt clusters. The analyzed cluster aggregate has an average composition of 52.5 at. % Fe from EDX spectrum taken with the spread beam.

tion (namely EDX spectrum taken with the spread beam).

Figure 3 shows the estimated lattice constants ( $a$ ) from the ED patterns. For  $C_{\text{Fe}} < 80\%$ , the  $a$  value of Fe–Pt clusters with a fcc structure clearly depends on the composition and linearly increases with decreasing Fe content. Moreover, it can be extrapolated to the lattice constant value of pure Pt metal (0.392 nm). This finding suggests that the Fe–Pt clusters formed in the present vapor phase were well alloyed. When  $C_{\text{Fe}} > 80\%$ , the ED measurement showed that the Fe–Pt clusters have a bcc–(Fe,Pt) structure (not shown here) and its lattice constant is about 0.287 nm. This result is also corresponding to our previous experimental result on the Co–Pt alloy clusters in which the clusters have a hcp–(Co,Pt) structure when Co content becomes larger than about 79%.<sup>14</sup>

We also carried out magnetic measurements on as-deposited  $\text{Fe}_x\text{Pt}_{1-x}$  alloy cluster assemblies ( $x \approx 0.35–0.7$ ). The results revealed that the as-deposited  $\text{Fe}_x\text{Pt}_{1-x}$  cluster-assembled films have lower blocking temperatures than room temperature and show a very small coercivity (a few tens of oersteds) at room temperature due to intercluster magnetic interaction. However, it is well known that chemically or-

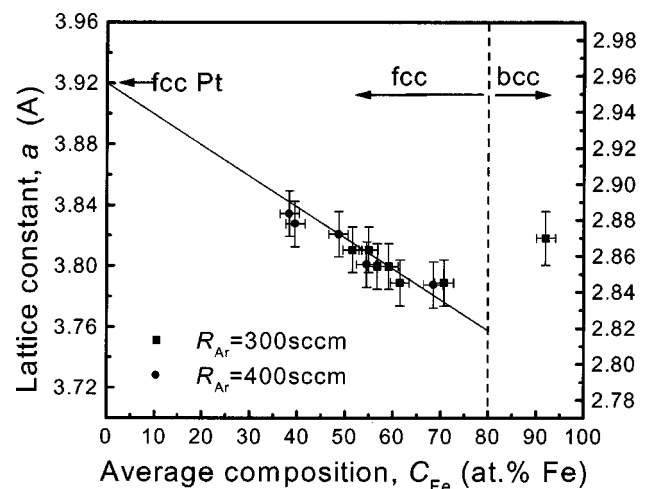


FIG. 3. Lattice constants of the Fe–Pt alloy clusters estimated by electron diffraction patterns as a function of the average composition ( $C_{\text{Fe}}$ ).

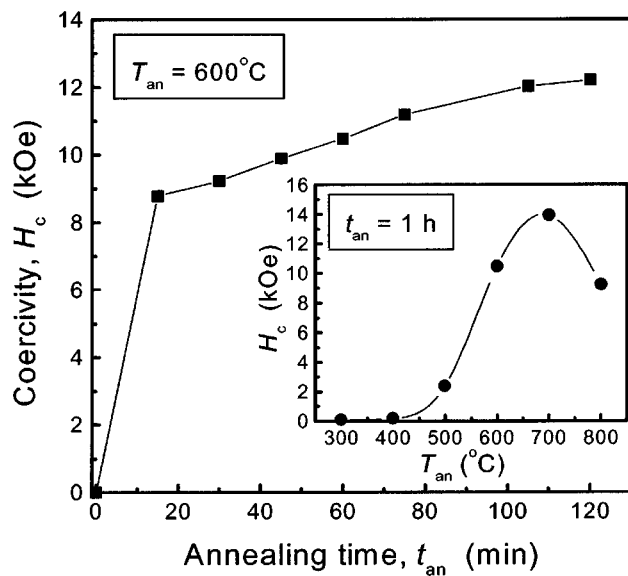


FIG. 4. Annealing time ( $t_{an}$ ) dependence of coercivity  $H_c$  for  $\text{Fe}_{49}\text{Pt}_{51}$  alloy cluster-assembled film with thickness of 50 nm annealed at  $600^\circ\text{C}$ . The inset shows  $H_c$  as a function of the annealing temperature  $T_{an}$ , with  $t_{an}$  fixed to be 1 h.

dered fct FePt clusters may show large coercivity originating from their large  $K_u$ .<sup>15</sup> The degree of ordering depends strongly on the annealing time and temperature. Figure 4 shows the coercivity ( $H_c$ ) variation of  $\text{Fe}_{49}\text{Pt}_{51}$  alloy cluster-assembled film with thickness of 50 nm as a function of the annealing time,  $t_{an}$ , at the annealing temperature of  $600^\circ\text{C}$ . The inset of Fig. 4 shows the annealing temperature ( $T_{an}$ ) dependence of the room-temperature  $H_c$ , where  $t_{an}$  was fixed as 1 h. As one can see in the inset, for  $T_{an} < 500^\circ\text{C}$ ,  $H_c$  did not exhibit obvious change. When  $T_{an}$  becomes higher than  $500^\circ\text{C}$ ,  $H_c$  first increases rapidly as  $T_{an}$  increases from 500 to  $700^\circ\text{C}$ , and then decreases dramatically with further increasing  $T_{an}$ . A peak value of  $H_c \sim 14$  kOe appears at  $700^\circ\text{C}$ . The similar result was also observed in Fe–Pt nanoparticle assemblies by chemical synthesis, probably resulting from excessive interparticle exchange coupling<sup>7</sup> due to particle–particle coalescence. As shown in Fig. 4, on the other hand,  $H_c$  value abruptly reached about 9 kOe after first 10 min annealing, and then increases gradually as  $t_{an}$  increases. This result also suggests that in the fcc disordered Fe–Pt clusters formed in the present vapor phase, Fe and Pt atoms have a homogeneous distribution so that the transformation towards a fct ordered phase occurred in such a short time, leading to a large  $H_c$ .

Typical hysteresis loops for the  $\text{Fe}_{49}\text{Pt}_{51}$  alloy cluster-assembled film with a thickness of 50 nm annealed at  $600^\circ\text{C}$  for 2 h, in directions both parallel and perpendicular to the film, are shown in Fig. 5. It is seen that for both directions, the loops show the same coercivity and almost the same shape, namely the same magnetic anisotropy.

In summary, we have employed a plasma-gas-condensation technique to produce nearly size-monodispersed disordered Fe–Pt alloy clusters which have the fcc structure in the composition range of 39–70 at. % Fe. It was observed that the composition of the clusters can be

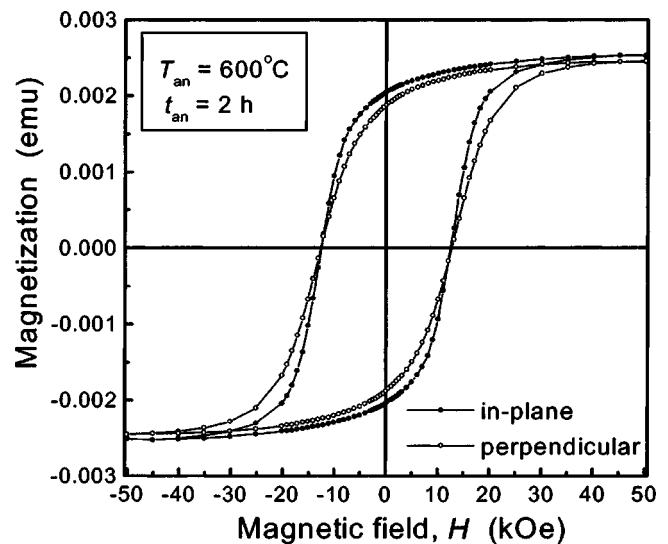


FIG. 5. Typical hysteresis loops for the  $\text{Fe}_{49}\text{Pt}_{51}$  alloy cluster-assembled film with a thickness of 50 nm annealed at  $600^\circ\text{C}$  for 2 h, in directions both parallel and perpendicular to the film.

controlled easily by changing the relative power of the two targets and the Ar gas flow rate. The experimental results also show that the Fe and Pt atoms are distributed homogeneously in the obtained alloy clusters which have a narrow distribution of the chemical composition. The optimal magnetic hardening or the chemical ordered fct FePt clusters can be achieved at proper annealing temperature and short annealing time.

This work has been supported by Grant-in-aid for Intellectual Cluster Project supported by the Ministry of Education, Science, Culture and Sports, Japan, Aichi Prefecture and Aichi Science and Technology Foundation. The authors appreciate H. Kurebayashi for his help on the sample preparation and Dr. S. Yamamuro for his helpful discussion.

<sup>1</sup> *Nanomaterials: Synthesis, Properties and Applications* (Institute of Physics, Bristol, 1996), edited by A. S. Edelstein and R. C. Cammarata.

<sup>2</sup> J. P. Liu, C. P. Luo, Y. Liu, and D. J. Sellmyer, *Appl. Phys. Lett.* **72**, 483 (1998).

<sup>3</sup> C. P. Luo, S. H. Liou, L. Gao, Y. Liu, and D. J. Sellmyer, *Appl. Phys. Lett.* **77**, 2225 (2000).

<sup>4</sup> H. Zeng, M. L. Yan, N. Powers, and D. J. Sellmyer, *Appl. Phys. Lett.* **80**, 2350 (2002).

<sup>5</sup> S. Sun, C. B. Murray, D. Weller, L. Folks, and A. Moser, *Science* **287**, 1989 (2000).

<sup>6</sup> S. Sun, E. E. Fullerton, D. Weller, and C. B. Murray, *IEEE Trans. Magn.* **37**, 1239 (2001).

<sup>7</sup> H. Zeng, S. Sun, T. S. Vedantam, J. P. Liu, Z.-R. Dai, and Z.-L. Wang, *Appl. Phys. Lett.* **80**, 2583 (2002).

<sup>8</sup> S. Stappert, B. Rellinghaus, M. Acet, and E. F. Wassermann, *Mater. Res. Soc. Symp. Proc.* **704**, 73 (2002).

<sup>9</sup> H. Haberland, M. Karrais, M. Mall, and Y. Thurner, *J. Vac. Sci. Technol. A* **10**, 3266 (1992).

<sup>10</sup> S. Yamamuro, K. Sumiyama, and K. Suzuki, *J. Appl. Phys.* **85**, 483 (1999).

<sup>11</sup> S. Yamamuro, K. Sumiyama, T. Hihara, and K. Suzuki, *J. Phys.: Condens. Matter* **11**, 3245 (1999).

<sup>12</sup> C.-M. Kuo, P. C. Kuo, and H.-C. Wu, *J. Appl. Phys.* **85**, 2264 (2002).

<sup>13</sup> P. T. L. Minh, N. P. Thuy, N. D. Van, and N. T. N. Chan, *J. Magn. Magn. Mater.* **239**, 335 (2002).

<sup>14</sup> T. J. Konno, S. Yamamuro, and K. Sumiyama, *J. Vac. Sci. Technol. B* **20**, 834 (2002).

<sup>15</sup> K. Watanabe and H. Masumoto, *J. Jpn. Inst. Met.* **48**, 930 (1984).